Helicase-DNA polymerase interaction is critical to initiate leading-strand DNA synthesis

Huidong Zhang[1], Seung-Joo Lee[1], Bin Zhu, Ngoc Q. Tran, Stanley Tabor, and Charles C. Richardson[2]

Department of Biological Chemistry and Molecular Pharmacology, Harvard Medical School, Boston, MA 02115

Interactions between gene 4 helicase and gene 5 DNA polymerase (gp5) are crucial for leading-strand DNA synthesis mediated by the replisome of bacteriophage T7. Interactions between the two proteins that assure high processivity are known but the interactions essential to initiate the leading-strand DNA synthesis remain unidentified. Replacement of solution-exposed basic residues (K587, K589, R590, and R591) located on the front surface of gp5 with neutral asparagines abolishes the ability of gp5 and the helicase to mediate strand-displacement synthesis. This front basic patch in gp5 contributes to physical interactions with the acidic C-terminal tail of the helicase. Nonetheless, the altered polymerase is able to replace gp5 and continue ongoing strand-displacement synthesis. The results suggest that the interaction between the C-terminal tail of the helicase and the basic patch of gp5 is critical for initiation of strand-displacement synthesis. Multiple interactions of T7 DNA polymerase and helicase coordinate replisome movement.

DNA polymerase-helicase interaction | strand-displacement DNA synthesis | T7 bacteriophage | T7 replisome

Fig. 1. Model of bacteriophage T7 replisome and crystal structure of gp5/trx bound to a primer template. (*A*) The T7 replisome consists of DNA polymerase gp5, the processivity factor thioredoxin, the gp4 helicase-primase, and the ssDNA-binding protein gp2.5. The helicase unwinds dsDNA to generate two ssDNA templates for both gp5/trx. The primase catalyzes the synthesis of RNA primers for the initiation of each Okazaki fragment. Gp2.5 coats the lagging ssDNA. (*B* and *C*) The basic patches at the surface of gp5/trx bound to a primer template (Protein Data Bank ID 1T8E; ref. 15). Four basic residues (K587, K589, R590, and R591, in blue, denoted as Fbp) are located within a solution-exposed patch facing the movement direction of gp5/trx along the ssDNA template. The basic H276, R278, and K281 in loop A and K302, K304, R307, and R310 in loop B of the trx-binding domain were denoted as TBDbp.

Bacteriophage T7 has a simple and efficient DNA replication system whose basic reactions mimic those of more complex replication systems (1). The T7 replisome consists of gene 5 DNA polymerase (gp5), the processivity factor, *Escherichia coli* thioredoxin (trx), gene 4 helicase-primase (gp4), and gene 2.5 ssDNA binding protein (gp2.5) (Fig. 1*A*). Gp5 forms a high-affinity complex with trx (gp5/trx) to increase the processivity of nucleotide polymerization (2). The C-terminal helicase domain of gp4 assembles as a hexamer and unwinds dsDNA to produce two ssDNA templates for leading- and lagging-strand gp5/trx. The N-terminal primase domain of gp4 catalyzes the synthesis of tetraribonucleotides that are used as primers for the lagging-strand gp5/trx. This gp5/trx also binds to helicase to form a replication loop containing the nascent Okazaki fragment. Gp2.5 coats the ssDNA to remove secondary structures and it also physically interacts with gp4 and gp5/trx, interactions essential for coordination of leading and lagging-strand synthesis (3).

Other DNA replication systems are generally more complicated than the T7 system. In *E. coli*, at least 13 proteins are required for a functional replisome and eight proteins are required in bacteriophage T4 infected cells (1, 4, 5). The two essential helicase and primase are separate proteins although they must physically interact to properly function (5). The additional proteins include processivity clamps and loading proteins. The existing T7 gp4 has usurped helicase and primase functions. The proofreading exonuclease activity resides within the N-terminal portion of gp5, whereas in the *E. coli* system it resides within ε subunit of the polymerase holoenzyme (5). Trx not only binds to gp5 to increase processivity but it also configures the trx-binding loop in gp5 for the binding of gp2.5 and gp4 (6). An interaction of the C-terminal tail of gp2.5 with gp5/trx is essential for the proper loading of gp5/trx and helicase at a nick (7).

In contrast to *E. coli* DNA polymerase III holoenzyme, the single polypeptide gp5 has acquired some other functions in addition to its polymerase and exonuclease activities. Without a requirement for accessory proteins, gp5/trx stably interacts with helicase during leading-strand DNA synthesis, providing a
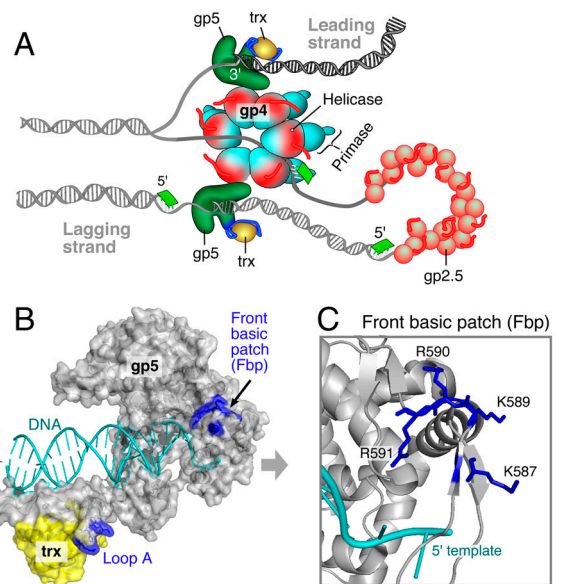
processivity of approximately 5 kb. Gp5/trx alone has a processivity of about 800 nt on ssDNA templates and the helicase has a processivity of 60–350 bp for DNA unwinding (1, 8, 9). DNA synthesis performed by gp5/trx provides a driving force for the helicase to unwind dsDNA, increasing the unwinding rate from 9.3 to 127 bp/s (10).

Gp5 has many solution-exposed charged residues that have the potential to interact with DNA and with other proteins (11). The trx-binding domain (TBD) of gp5 contains two basic patches located in loops A and B (denoted as TBD basic patch, TBDbp, Fig. 1*B*). Gp4 and gp2.5 have acidic C-terminal tails, both of which bind to loops A and B in gp5/trx (6, 12). This electrostatic

interaction of gp5/trx with gp4 serves as a reservoir for gp5/trx that transiently dissociates from the primer template during replication (12, 13), increasing the processivity from the 5 kb per binding event to greater than 17 kb. The exchange of DNA polymerases without affecting processivity was first described for the T4 replication system (14).

Another basic patch (K587, K589, R590, and R591) is located at the front side of gp5 facing its movement direction along the ssDNA template (denoted as front basic patch, Fbp) (16) (Fig. 1 *B* and *C*). In a previous study, we found that T7 lacking gene 5 cannot grow in cells containing gp5 in which these basic residues were replaced with neutral residues, Asn (16). Despite this detrimental effect on T7 growth, the only defect observed was a threefold decrease in polymerase activity on ssDNA templates and a reduced processivity. One reasonable explanation for the lethal effect of these mutations in gene 5 is an alteration in a binding site for one or more of the other T7 replication proteins. Indeed, in the current study, we show that gp5 in which these four residues are neutralized by replacement with Asn (gp5-Fbp$_{neu}$) has a markedly lower binding affinity for the gene 4 helicase and cannot initiate strand-displacement synthesis with T7 helicase. Our experiments also show that there are multiple interactions of gp5/trx with helicase, each designed for separate steps in replication.

Results

Neutralization of a Basic Patch in T7 DNA Polymerase (gp5-Fbp$_{neu}$) Abolishes Its Ability to Mediate Strand-Displacement DNA Synthesis. A solution-exposed patch (Fbp) with four basic residues (K587, K589, R590, and R591) is located near the 5′ overhang of the ssDNA template in gp5 (Fig. 1*C*). T7 lacking gene 5 cannot grow in cells expressing gp5 in which these residues are neutralized by replacement with Asn (16). This altered gp5 is designated gp5-Fbp$_{neu}$. Despite this detrimental effect on T7 growth, the rate of DNA synthesis catalyzed by gp5-Fbp$_{neu}$/trx on a primed ssDNA is reduced only threefold (Fig. S1*A*) as previously shown (16).

In the presence of T7 gene 4 helicase, gp5/trx catalyzes strand-displacement DNA synthesis using an M13 dsDNA bearing a 5′-ssDNA tail to assemble gp4 (Fig. 2). Gp5-Fbp$_{neu}$/trx does not mediate the synthesis in the presence of gp4 over a large range of concentrations of gp5/trx and gp4 (Fig. 2). Extending the peri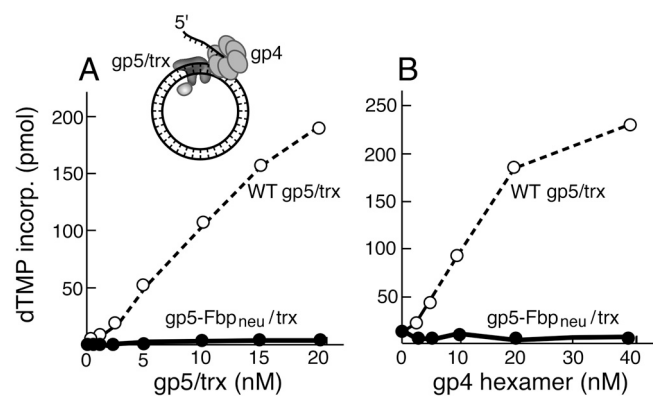od of incubation does not result in any detectable DNA synthesis (Fig. S1*B*). Because the concentrations of DNA polymerase are similar in the assays presented in both Fig. 2*A* and Fig. S1*A*, the lack of strand-displacement synthesis by gp5-Fbp$_{neu}$ is not due to its reduced polymerase activity.

The primase domain of gp4 catalyzes the synthesis of RNA primer for gp5/trx to initiate DNA synthesis on ssDNA template. gp5-Fbp$_{neu}$/trx mediates RNA-dependent DNA synthesis on M13 ssDNA with gp4 approximately one-third to one-half as well as does wild-type gp5/trx (Fig. S2). Thus neutralization of this basic patch in gp5 does not appear to be a defect in the polymerization activity when using a de novo synthesized or transferred RNA primer.

The Fbp and the TBD Basic Patch in Gp5 Independently Interact with the C-terminal Tail of Gp4. Physical interactions between gp4 and gp5/trx are required for the coordination of DNA unwinding and DNA synthesis. We have previously shown that the C-terminal tail of gp4 interacts with the loops A and B located in the TBD of gp5 (6). Removal of the C-terminal tail or neutralization of its acidic residues abolishes the ability of gp4 to mediate strand-displacement synthesis together with gp5/trx (17, 18). Neutralization of the charges in loops A and B of the TBD weakens the binding affinity of gp5 with gp4 and reduces the processivity of strand-displacement synthesis from 17 to 5 kb (12). The loss of strand-displacement synthesis with gp5-Fbp$_{neu}$/trx described above suggests that neutralization of this Fbp in gp5 also alters its interaction with gp4, which is likely to also involve the C-terminal tail of gp4. Therefore, we have examined the interaction of gp4 or gp4-ΔC17 lacking the entire C-terminal tail with gp5-Fbp$_{neu}$/trx or with gp5-TBDbp$_{neu}$/trx using surface plasmon resonance (SPR). The basic residues in two loops of TBD (Fig. 1*B*) were replaced with Ala in gp5-TBDbp$_{neu}$.

In the SPR experiments, gp4 or gp4-ΔC17 (7,400 response units, RU) were immobilized to the CM-5 sensor chip (scheme in Fig. 3*A*). The gp5/trx variants were then flowed over the chip and the change in RU was recorded. We used gp5 exo$^-$ in this experiment for consistency with subsequent experiments involving DNA. Both gp5-Fbp$_{neu}$/trx and gp5-TBDbp$_{neu}$/trx bind to gp4 less well relative to wild-type gp5/trx (Fig. 3*B*). Compared with our previous report (12), considerably more gp4 was immobilized to the chip allowing for observation of the binding of both the variant gp5/trx. Elimination of the C-terminal tail of gp4 abolishes all binding of each gp5/trx (Fig. 3*B*). Therefore, the acidic C-terminal tail of gp4 interacts with the Fbp and the TBDbp of gp5.

In order to compare quantitatively the binding affinities of gp5/trx, gp5-Fbp$_{neu}$/trx, and gp5-TBDbp$_{neu}$/trx to gp4, varying concentrations of each protein were flowed over gp4 (5,200 RU, Fig. 3*C* and Fig. S3). The binding affinity (K_d) and the maximal amount of binding (RU$_{max}$) were fitted using the steady-state model as described previously (6) (Fig. 3*D* and Fig. S3). All three gp5/trx have a similar affinity (K_d of 90 nM) for gp4 (Fig. 3*E*). We conclude that the C-terminal tail of gp4 has approximately the same affinity for either the Fbp or the TBDbp of gp5. Furthermore, only one patch in gp5/trx binds to the C-terminal tail of a gp4 within a hexamer; but not both patches bind the C-terminal tails simultaneously. The maximal binding of the two altered gp5/trx to gp4 is approximately one-third of that obtained with wild-type gp5/trx. It should be noted that K_d represents binding affinity between two sites in two proteins and RU$_{max}$ represents the maximal binding capacity. When gp5 is flowed over gp4 on the sensor chip, wild-type gp5 with two binding sites available has a higher chance to be captured by gp4 than either of the altered gp5 (Fig. S4).

We have examined the physical interaction of gp4 bound to ssDNA with gp5-Fbp$_{neu}$/trx or gp5-TBDbp$_{neu}$/trx (Fig. S5). With nonhydrolyzable β,γ-CH$_2$-dTTP, a stable ssDNA-gp4 binary

Fig. 2. Gp5-Fbp$_{neu}$/trx cannot mediate strand-displacement DNA synthesis with gp4. The "neu" denotes the replacement of the basic patch with neutral residue Asn. (*A*) The reaction mixture contained 10 nM M13 dsDNA template (*Inset*), 0.3 mM of dATP, dGTP, dCTP, and [³H] dTTP (10 cpm/pmol), 200 nM monomer of gp4, and varying concentration of the indicated gp5/trx in the buffer A [40 mM Tris • HCl(pH 7.5), 10 mM MgCl$_2$, 10 mM DTT, and 50 mM potassium glutamate]. After incubation at 37 °C for 20 min, the reaction was terminated and the amount of [³H] dTMP incorporated into DNA was measured as described in *Materials and Methods*. (*B*) The reaction was similar to *A* except for using a constant amount of gp5/trx (20 nM) and varying concentrations of gp4 hexamer.
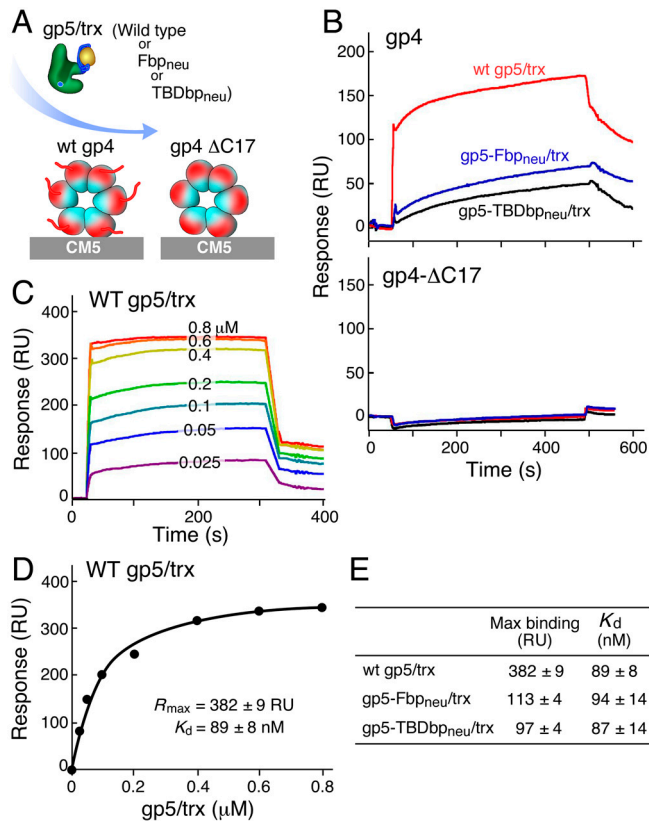
Fig. 3. The Fbp and TBDbp of gp5 independently interact with the C-terminal tail of gp4. (*A*) Scheme for measuring the affinity of gp5/trx to gp4 by SPR analysis, as described in *Materials and Methods*. Gp4 or gp4-ΔC17 was immobilized to the CM-5 chip and gp5/trx was flowed over the bound gp4. The neu denotes the replacement of the basic patch with neutral residues. (*B*) Each 0.25 μM of indicated gp5 exo⁻ and 5 μM trx were flowed over the immobilized gp4 or gp4-ΔC17 (7,400 RU) and the change in RU was recorded. (*C*) Sensorgrams for the binding of increasing concentrations of wild-type gp5/trx to the immobilized gp4 (5,200 RU). Sensorgrams for gp5-Fbp$_{neu}$/trx and gp5-TBDbp$_{neu}$/trx are shown in Fig. S3. (*D*) The binding affinities of wild-type gp5/trx to gp4 were determined using the steady-state average response at each concentration shown in *C*. The solid line represents the theoretical curve calculated from the steady-state fit model (Biacore). (*E*) The maximal binding amount (RU$_{max}$) and the K_d values for binding of each of gp5/trx to gp4 were obtained from the data shown in Fig. 3 *C* and *D* and Fig. S3.

complex (18) is formed (lanes 1 and 5). Addition of gp5/trx to the binary complex leads to the formation of a stable ternary complex (lanes 2 and 6). The amount of complex is greater with gp4 than that with gp4-ΔC17. Both the altered gp5/trx form less ternary complex with gp4 than does wild-type gp5/trx (lanes 3 and 4 vs. 2), suggesting that the Fbp and TBDbp are important in interactions with gp4. Similarly, both the altered gp5/trx are deficient in forming a ternary complex with gp4-ΔC17 (lanes 7 and 8 vs. 6). Comparison of lanes 2–4 (with gp4) and 6–8 (with gp4-ΔC17) also suggests that the C-terminal tail of gp4 has interactions with both the Fbp and TBDbp. The assays in Fig. 3 and Fig. S5 are not same because gp4 is randomly bound to the chip in Fig. 3 and is bound to ssDNA as a hexamer in Fig. S5.

Multiple Modes of Interactions Between Gp4 and Gp5/trx in a Replication Complex. During leading-strand DNA synthesis, the gp4 hexamer encircles the lagging ssDNA, whereas gp5/trx extends primer on the leading-strand template (Fig. 1*A*). Terminating the primer with a ddATP and providing the next dGTP specified by the template yield a stable gp5/trx-gp4 complex that mimics ongoing leading-strand synthesis (6) (Fig. 4*A*). In order to deter-
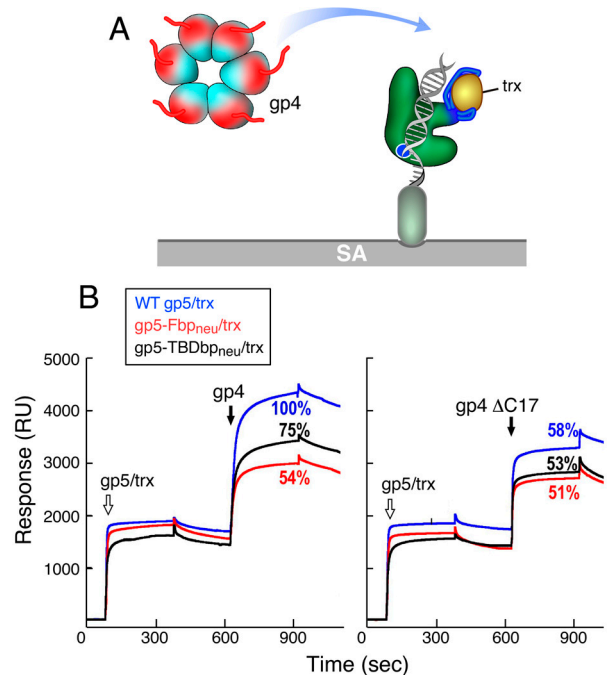
Fig. 4. Multiple modes of interactions between gp4 and gp5/trx in a replication complex. (*A*) Scheme for measuring interaction of gp4 with gp5/trx bound to a primer template, as described in *Materials and Methods*. An annealed primer template was immobilized on the chip (600 RU). Gp5/trx forms a stable complex with the primer template when the ddATP is at 3′ terminus of the primer and the incoming dGTP is present (6). (*B*) Binding of gp4 or gp4-ΔC17 to each of gp5/trx-DNA complex. The neu denotes the replacement of the basic patch with neutral residues. Gp5, gp5-Fbp$_{neu}$, or gp5-TBDbp$_{neu}$ (0.25 μM) was injected with 10 μM trx in the flow buffer C containing 1 mM dGTP and 10 μM ddATP. Then 0.8 μM monomer of gp4 or gp4-ΔC17 was flowed in the same buffer C containing 0.1 mM ATP and 2 mM dGTP. The percentages denote the relative binding affinity of gp4 or gp4-ΔC17 with each gp5/trx, normalized against the binding affinity of gp4 to wild-type gp5/trx.

mine if the Fbp participates in this stable interaction, the binding of gp4 with gp5-Fbp$_{neu}$/trx bound to a primer template was examined using SPR.

In this experiment (Fig. 4*B*), gp5/trx, gp5-Fbp$_{neu}$/trx, and gp5-TBDbp$_{neu}$/trx all bind stably and equally well to the immobilized DNA in the presence of ddATP and dGTP. Gp5 exo⁻ was used to avoid degradation of DNA. Upon flowing gp4 over the immobilized complex, all gp5/trx form equally stable complexes with gp4 due to the slow dissociation after the injection of gp4 (Fig. 4*B*). In control, we found no detectable binding of gp4 to the immobilized DNA alone (6). To compare the binding affinity of gp4 to each gp5/trx, the maximal RU of gp4 bound to each gp5/trx-DNA complex was divided by the maximal RU of gp5/trx bound to the DNA. These binding affinities were normalized against that for binding of gp4 to wild-type gp5/trx. Gp4 bound to gp5-Fbp$_{neu}$/trx or gp5-TBDbp$_{neu}$/trx at 54% and 75%, respectively, of the level observed for wild-type gp5/trx. Both the Fbp and the TBDbp of gp5 contribute to the interaction with gp4.

In order to determine if the C-terminal tail of gp4 interacts with gp5 bound to DNA, gp4-ΔC17 lacking the C-terminal tail was also examined. The C-terminal tail of gp4 is most likely quite flexible in solution and in fact does not diffract in the crystal structure (19). Removal of the free tail does not change the surface of gp4, thus does not create an artificial interaction with gp5/trx. Gp4-ΔC17 forms a stable complex with all of gp5/trx-DNA complexes (Fig. 4*B*). The relative binding affinities of gp4-ΔC17 to each gp5/trx were also calculated as described above and normalized against binding of gp4 to wild-type gp5/trx. Gp4-ΔC17 shows similar binding to each of the gp5/trx variants,

approximately 55% of the level observed for the binding wild-type gp4 to wild-type gp5/trx (Fig. 4B), independent on the C-terminal tail of gp4 or the basic regions on gp5. In contrast, the binding of gp4 to gp5-Fbp$_{neu}$/trx (54%) or gp5-TBDbp$_{neu}$/trx (75%) is weaker than the binding of gp4 to wild-type gp5/trx (100%), resulting from the electrostatic binding involving the C-terminal tail of gp4 and two basic regions on gp5. Taken together, these results support at least three modes of binding of gp4 with gp5/trx when gp5/trx is bound to a primer template. The C-terminal tail of gp4 interacts with the Fbp and TBDbp of gp5. More than half of the binding is contributed by a third unidentified interaction.

Gp5-Fbp$_{neu}$/trx Can Exchange with Gp5/trx at a Replication Fork and Mediate Ongoing Leading-Strand DNA Synthesis. Although the C-terminal tail of gp4 interacts with both the Fbp and the TBD basic patch, there is no reason to assume the same consequences of these interactions. The interaction of the C-terminal tail of gp4 with TBDbp of gp5 serves to capture dissociating gp5/trx and as a reservoir for gp5/trx (12). Elimination of this interaction reduced the processivity of nucleotide polymerization but did not affect its rate with gp4. In contrast, elimination of the interaction of the C-terminal tail of gp4 with the Fbp of gp5 abolished all strand-displacement synthesis. One explanation might be an inability of gp5-Fbp$_{neu}$/trx to form an initial functional complex with gp4.

Gp5/trx in solution can exchange with the replicating gp5/trx during strand-displacement synthesis in the presence of gp4 (20). Gp5/trx incorporates chain terminating dideoxynucleotides (ddNTP) with high efficiency (21). However, gp5-Y526F, in which tyrosine 526 is replaced with phenylalanine, discriminates several thousandfold against ddNTPs (21). Based on this marked difference, we have examined the ability of gp5-Fbp$_{neu}$/trx to exchange with gp5-Y526F/trx during ongoing strand-displacement synthesis.

In the experiment (Fig. 5A), DNA synthesis was initiated by gp5-Y526F/trx and gp4 on M13 dsDNA template (Inset). The addition of ddGTP to this reaction did not affect DNA synthesis because gp5-Y526F discriminates against ddNTPs (black curve). In a separate reaction, after 1 min of DNA synthesis, a 10-fold excess of wild-type gp5/trx was added to the reaction and the rate of DNA synthesis was approximately twofold of that observed with gp5-Y526F/trx. The increased rate, in itself, is indicative of exchange of DNA polymerases at the replication fork because wild-type gp5/trx is approximately twice as active as gp5-Y526F/trx (20). When ddGTP was added to this reaction at 2 min of incubation (after the addition of excess gp5/trx), DNA synthesis ceased because gp5/trx incorporates ddNTPs as well as dNTPs (red curve).

The exchange assays with gp5-Fbp$_{neu}$/trx were performed as described above except for using gp5-Fbp$_{neu}$/trx instead of wild-type gp5/trx (Fig. 5B). Upon addition of an excess of gp5-Fbp$_{neu}$/trx and ddGTP to the ongoing reaction, all DNA synthesis ceased (red curve), indicating that gp5-Fbp$_{neu}$/trx replaced gp5-Y526F/trx at the replication fork. More important is the continued DNA synthesis upon addition of excess gp5-Fbp$_{neu}$/trx but without ddGTP (blue curve). The rate of DNA synthesis is essentially the same as that observed with gp5-Y526F/trx alone (black curve), and twofold lower than that observed with wild-type gp5/trx. Therefore, the inability of gp5-Fbp$_{neu}$/trx to perform strand-displacement synthesis (Fig. 2) is due to a defect in the initiation of this synthesis.

Discussion

The C-terminal tail of gp4 interacts with both of the basic regions on gp5, but the consequences of those interactions are quite different. Gp5-TBDbp$_{neu}$/trx can initiate strand-displacement DNA synthesis with T7 helicase with only a twofold decrease in efficiency (12). The interaction of the C-terminal tail of gp4
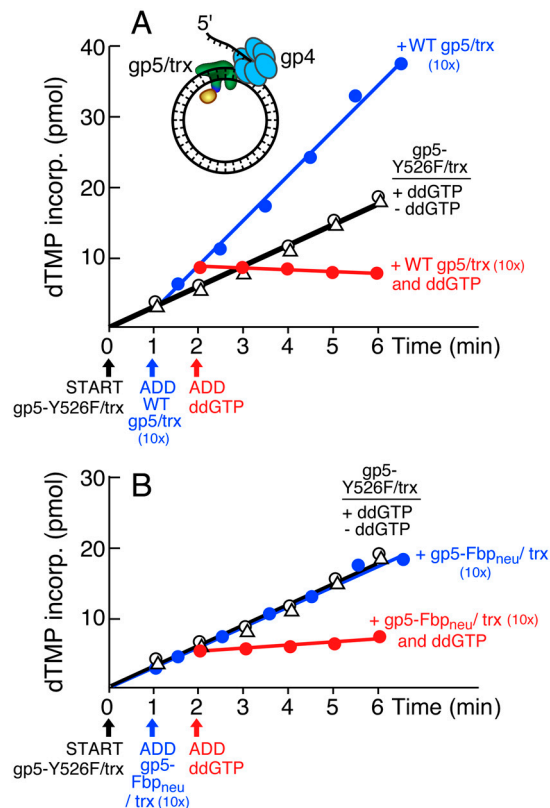

Fig. 5. Gp5-Fbp$_{neu}$/trx can exchange with gp5/trx at the replication fork and mediate ongoing leading-strand DNA synthesis. (A) Exchange of gp5-Y526F/trx with wild-type gp5/trx during leading-strand DNA synthesis was performed as described in Materials and Methods. The reactions contained 2 nM M13 dsDNA template (see Inset), 100 nM monomer of gp5-Y526F/trx, 16 nM gp5-Y526F/trx, 0.5 mM each dATP, dGTP, dCTP, and [³H] dTTP (10 cpm/pmol) in the buffer A [40 mM Tris • HCl (pH 7.5), 10 mM MgCl$_2$, 10 mM DTT, and 50 mM potassium glutamate]. After 1 min, a 10-fold excess of wild-type gp5/trx (160 nM) was added, followed by the addition of 50 μM ddGTP at 2 min. The amount of [³H] dTMP incorporated into the DNA was determined (red). As controls, the reaction mediated by only gp5-Y526F/trx with or without the addition of ddGTP (black), or together with a 10-fold excess of wild-type gp5/trx without the addition of ddGTP (blue) is also shown. (B) Exchange of gp5-Y526F/trx with gp5-Fbp$_{neu}$/trx during leading-strand DNA synthesis was carried as described in A except for using gp5-Fbp$_{neu}$/trx instead of wild-type gp5/trx.

with the TBDbp of gp5 increases the processivity of the replisome but does not affect the rate of leading-strand synthesis. Elimination of this interaction abolishes DNA polymerase exchange during leading-strand DNA synthesis. In the present study, we show that a solution-exposed Fbp in gp5 also interacts with the C-terminal tail of gp4. Elimination of the charges in this patch is lethal for the growth of T7 (16) yet the polymerase activity of this altered gp5 (gp5-Fbp$_{neu}$) is reduced only threefold. Importantly, gp5-Fbp$_{neu}$/trx is unable to mediate leading-strand synthesis in conjunction with T7 helicase. Nonetheless, gp5-Fbp$_{neu}$/trx can support DNA polymerase exchange during leading-strand DNA synthesis and continue ongoing DNA synthesis. Thus the defect in gp5-Fbp$_{neu}$ appears to be an inability to initiate strand-displacement synthesis with the helicase.

Both the electrostatic interactions involving the TBDbp and the Fbp contribute to the binding of gp4 to gp5/trx. Furthermore, there is clearly a third unidentified interaction that accounts for more than half of the binding observed in the replication complex that does not involve the C-terminal tail of gp4 and hence probably neither of the two basic sites in gp5. This third interaction is essential for the high processivity of the replisome observed
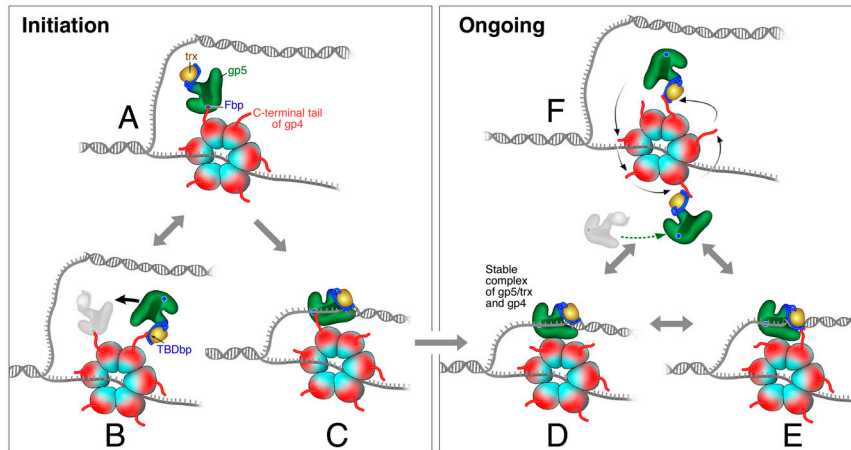
Fig. 6. Specific interactions of T7 DNA polymerase and helicase coordinate each step in DNA replication. (*A*) The gp4 assembles as a hexamer on the lagging-strand DNA. Gp5/trx is recruited to the replication fork by an initial interaction with the C-terminal tail of gp4 through its Fbp. (*B*) Gp5/trx can also initially bind to gp4 via its two basic loops in the TBD (TBDbp). However, prior to loading onto the primer template, gp5/trx must first transfer its binding site to the Fbp site as in *A*. (*C*) The interaction of the Fbp of gp5 with the C-terminal tail of helicase facilitates the loading of gp5/trx to the primer template. (*D*) During ongoing leading-strand synthesis, gp5/trx and gp4 form a stable complex, independent of the C-terminal tail of gp4 or the basic patches in gp5. (*E*) If gp5/trx transiently dissociates from the primer template, an interaction of the C-terminal tail with the TBDbp retains it within the replisome where gp5/trx can rapidly return to the primer template. The interaction of Fbp with gp4 is not necessary. (*F*) The C-terminal tails of the gp4 hexamer not only bind any dissociating gp5/trx but they also accommodate additional gp5/trx through interactions with the TBDbp of gp5. Any of these gp5/trx can be reloaded onto the primer template without involvement of the Fbp.

during leading-strand DNA synthesis. Gp5/trx alone has a processivity of only 800 nt on ssDNA but a processivity of 5 kb during leading-strand DNA synthesis when coupled to the helicase (1).

A model for the multiple interactions of gp5/trx and gp4 helicase is presented in Fig. 6. Gp4 hexamer stably assembles on the lagging-strand template as evidenced by the extremely low dissociation rate of 0.002 s^{-1} (22). Gp5/trx binds relatively weaker to the primer template with a dissociation rate of 0.2 s^{-1} (23). We propose that gp5/trx joins the replisome by first binding to the C-terminal tail of helicase through its Fbp (Fig. 6*A*). This Fbp faces the direction of movement of gp5/trx-gp4, thus providing a high probability of interaction with the gp4 hexamer. Furthermore, this initial interaction is supported by the SPR and gel mobility shift data. Thus gp5-Fbp$_{neu}$/trx, lacking this basic patch, cannot participate in this initial step. Once bound to the helicase, gp5/trx can transfer to the primer template (Fig. 6*C*). This interaction has been observed using SPR in which gp4 interacts with gp5/trx bound to a primer template.

Alternatively, gp5/trx initially binds the C-terminal tail of gp4 via its TBDbp (Fig. 6*B*), an interaction supported by the gel mobility shift data. Gp5-TBDbp$_{neu}$/trx can initiate strand-displacement synthesis with gp4 (12) showing that this interaction is not essential for the loading of gp5/trx to the primer-template/helicase complex. Therefore, gp5/trx bound to one subunit of gp4 hexamer via the TBDbp should transfer to bind another subunit via the Fbp (Fig. 6 *A* and *B*).

Once gp5/trx is engaged in the polymerization of nucleotides, there is a switch to a stable interaction between gp5/trx and gp4 that does not involve the C-terminal tail of gp4 or the two basic regions in gp5 (Fig. 6*D*). This stable interaction has been observed by SPR (Fig. 4*B*). The interaction between gp4 and the TBDbp of gp5 increases the processivity from approximately 5 kb to greater than 17 kb (12). We have proposed that, upon dissociation, on average every 5 kb, gp5/trx is transiently captured by the C-terminal tail of gp4 in an interaction with the TBDbp of gp5 (Fig. 6*E*). Gp5/trx that escapes into solution can also be captured by the helicase that serves as a reservoir (Fig. 6*F*). When gp5/trx bound to gp4 is reloaded onto the primer template, the Fbp is not required. We speculate that gp5/trx bound to gp4 maintains an orientation suitable for reloading onto the 3′ terminus of the leading strand (Fig. 6*F*). However, gp5/trx from solution

requires the interaction of its Fbp with the C-terminal tail of gp4 to load onto the replication fork in the initiation step (Fig. 6*A*).

The T7 replisome also contains the ssDNA binding protein gp2.5. Gp2.5 with an acidic C-terminal tail (3) can bind to the two basic loops in the TBD of gp5 (6). We have found that both the Fbp and TBDbp physically interact with gp2.5 examined by SPR (Fig. S6). However, gp5-Fbp$_{neu}$/trx still can not initiate strand-displacement synthesis even in the presence of gp2.5 (data not shown).

The acidic C-terminal tail of gp4 obviously plays important roles in the T7 replisome. However, this acidic C-terminal tail is not always conserved in other replicative helicases (18). Furthermore, accessory proteins found in other systems such as *E. coli* and bacteriophage T4 are not required in the T7 system. In *E. coli*, the $\gamma_3\delta\delta'\chi\psi$ clamp loader loads the β sliding clamp onto the DNA, and then the clamp loader is ejected from the clamp after hydrolysis of ATP. The free β-clamp is then ready for loading DNA polymerase III onto DNA (24). A similar clamp-loader complex, gp44/gp62, encoded by phage T4, loads the gene 45 clamp onto duplex DNA. Then DNA polymerase gp43 displaces the clamp loader and loads onto DNA (25). A replication factor C complex serves as a clamp loader to load proliferating cell nuclear antigen onto DNA in eukaryotes and archaea (4). In the T7 system, processivity of the polymerase is conferred by trx bound to gp5, such that trx resides on DNA as one part of the clamp. If one envisions the combination of gp5 and trx as a clamp, then the interaction of the C-terminal tail of gp4 with the Fbp can be considered a clamp-loading process.

Loading helicase onto ssDNA also requires a loader protein (26). In *E. coli*, the DnaB helicase loader loads helicase onto ssDNA and in phage T4 the same function is provided by the gene 59 protein. In the T7 system, assembly of the helicase may proceed through the loss of one subunit from the heptameric form (27). In *E. coli*, the τ subunit in $\tau_3\delta\delta'\chi\psi$ clamp-loader complex reserves DNA polymerase III and helicase at the replication fork (28). The β sliding clamp also plays a role in recruitment of DNA polymerases to the primer template (29). In T7, the stable interaction between helicase and gp5 can retain the two DNA polymerases at the replication fork. The interaction of the C-terminal tail of helicase with the basic loops in the TBD of gp5 can recap-

ture any dissociating DNA polymerase and return it to the primer template.

In conclusion, we have described multiple modes of interactions between the helicase and the DNA polymerase of bacteriophage T7. Each interaction is designed for a specific function during assembly and movement of the replisome. We hope the understanding of these processes in the T7 replication system will provide information on these more complex systems and how they evolved.

Materials and Methods

Details of assay procedures are shown in the *SI Text*. In the SPR and gel mobility shift assays, gp5 exo⁻ and trx were added separately. In all reaction assays, the holoenzyme gp5/trx was used.

1. Hamdan SM, Richardson CC (2009) Motors, switches, and contacts in the replisome. *Annu Rev Biochem* 78:205–243.
2. Tabor S, Huber HE, Richardson CC (1987) *Escherichia coli* thioredoxin confers processivity on the DNA polymerase activity of the gene 5 protein of bacteriophage T7. *J Biol Chem* 262:16212–16223.
3. Marintcheva B, Hamdan SM, Lee SJ, Richardson CC (2006) Essential residues in the C terminus of the bacteriophage T7 gene 2.5 single-stranded DNA-binding protein. *J Biol Chem* 281:25831–25840.
4. Johnson A, O'Donnell M (2005) Cellular DNA replicases: Components and dynamics at the replication fork. *Annu Rev Biochem* 74:283–315.
5. Benkovic SJ, Valentine AM, Salinas F (2001) Replisome-mediated DNA replication. *Annu Rev Biochem* 70:181–208.
6. Hamdan SM, et al. (2005) A unique loop in T7 DNA polymerase mediates the binding of helicase-primase, DNA binding protein, and processivity factor. *Proc Natl Acad Sci USA* 102:5096–5101.
7. Ghosh S, Marintcheva B, Takahashi M, Richardson CC (2009) C-terminal phenylalanine of bacteriophage T7 single-stranded DNA-binding protein is essential for strand-displacement synthesis by T7 DNA polymerase at a nick in DNA. *J Biol Chem* 284:30339–30349.
8. Lee JB, et al. (2006) DNA primase acts as a molecular brake in DNA replication. *Nature* 439:621–624.
9. Jeong YJ, Levin MK, Patel SS (2004) The DNA-unwinding mechanism of the ring helicase of bacteriophage T7. *Proc Natl Acad Sci USA* 101:7264–7269.
10. Stano NM, et al. (2005) DNA synthesis provides the driving force to accelerate DNA unwinding by a helicase. *Nature* 435:370–373.
11. Doublie S, Tabor S, Long AM, Richardson CC, Ellenberger T (1998) Crystal structure of a bacteriophage T7 DNA replication complex at 2.2 angstrom resolution. *Nature* 391:251–258.
12. Hamdan SM, et al. (2007) Dynamic DNA helicase-DNA polymerase interactions assure processive replication fork movement. *Mol Cell* 27:539–549.
13. Loparo JL, Kulczyk AW, Richardson CC, van Oijen AM (2011) Observing polymerase exchange by simultaneous measurements of replisome composition and function at the single-molecule level. *Proc Natl Acad Sci USA* 108:3584–3589.
14. Yang J, Zhuang Z, Roccasecca RM, Trakselis MA, Benkovic SJ (2004) The dynamic processivity of the T4 DNA polymerase during replication. *Proc Natl Acad Sci USA* 101:8289–8294.
15. Brieba LG, et al. (2004) Structural basis for the dual coding potential of 8-oxoguanosine by a high-fidelity DNA polymerase. *EMBO J* 23:3452–3461.
16. Lee SJ, Chowdhury K, Tabor S, Richardson CC (2009) Rescue of bacteriophage T7 DNA polymerase of low processivity by suppressor mutations affecting gene 3 endonuclease. *J Virol* 83:8418–8427.
17. Notarnicola SM, Mulcahy HL, Lee J, Richardson CC (1997) The acidic carboxyl terminus of the bacteriophage T7 gene 4 helicase/primase interacts with T7 DNA polymerase. *J Biol Chem* 272:18425–18433.
18. Lee SJ, Marintcheva B, Hamdan SM, Richardson CC (2006) The C-terminal residues of bacteriophage T7 gene 4 helicase-primase coordinate helicase and DNA polymerase activities. *J Biol Chem* 281:25841–25849.
19. Singleton MR, Sawaya MR, Ellenberger T, Wigley DB (2000) Crystal structure of T7 gene 4 ring helicase indicates a mechanism for sequential hydrolysis of nucleotides. *Cell* 101:589–600.
20. Johnson DE, Takahashi M, Hamdan SM, Lee SJ, Richardson CC (2007) Exchange of DNA polymerases at the replication fork of bacteriophage T7. *Proc Natl Acad Sci USA* 104:5312–5317.
21. Tabor S, Richardson CC (1995) A single residue in DNA polymerases of the *Escherichia coli* DNA polymerase I family is critical for distinguishing between deoxyribonucleotides and dideoxyribonucleotides. *Proc Natl Acad Sci USA* 92:6339–6343.
22. Kim DE, Narayan W, Patel SS (2002) T7 DNA helicase: A molecular motor that processively and unidirectionally translocates along single-stranded DNA. *J Mol Biol* 321:807–819.
23. Patel SS, Wong I, Johnson KA (1991) Pre-steady-state kinetic analysis of processive DNA replication including complete characterization of an exonuclease-deficient mutant. *Biochemistry* 30:511–525.
24. O'Donnell M (2006) Replisome architecture and dynamics in *Escherichia coli. J Biol Chem* 281:10653–10656.
25. Perumal SK, Yue H, Hu Z, Spiering MM, Benkovic SJ (2010) Single-molecule studies of DNA replisome function. *Biochim Biophys Acta* 1804:1094–1112.
26. Weigel C, Seitz H (2006) Bacteriophage replication modules. *FEMS Microbiol Rev* 30:321–381.
27. Crampton DJ, Ohi M, Qimron U, Walz T, Richardson CC (2006) Oligomeric states of bacteriophage T7 gene 4 primase/helicase. *J Mol Biol* 360:667–677.
28. McInerney P, Johnson A, Katz F, O'Donnell M (2007) Characterization of a triple DNA polymerase replisome. *Mol Cell* 27:527–538.
29. Indiani C, McInerney P, Georgescu R, Goodman MF, O'Donnell M (2005) A sliding-clamp toolbelt binds high-and low-fidelity DNA polymerases simultaneously. *Mol Cell* 19:805–815.

BIOCHEMISTRY